

Band-gap narrowing in heavily defect-doped ZnO

Alain P. Roth, James B. Webb, and Digby F. Williams

Semiconductor Group, Division of Chemistry, National Research Council, Ottawa, K1A 0R6 Canada

(Received 2 December 1981; revised manuscript received 1 March 1982)

Band-gap narrowing has been measured optically for semiconducting zinc-oxide films. All films were *n* type with carrier densities of $5 \times 10^{17} - 2 \times 10^{20} \text{ cm}^{-3}$. The narrowing appeared suddenly at $n \sim 2 \times 10^{19} \text{ cm}^{-3}$, a carrier density consistent with that expected for the onset of a semiconductor-metal transition. However the gap-shrinkage dependence on carrier concentration was not $n^{1/3}$ as expected from predictions based on an electron-gas model, but could be described by the same empirical relation proposed for Si:As and Si:B.

The effect of increasing carrier density on the properties of heavily doped semiconductors, particularly silicon, germanium, and gallium arsenide, has received considerable attention in recent years.¹⁻⁵ Much of the interest has come from the importance of heavily doped Si in current device technology and few other materials have been studied. Nevertheless, theoretical evaluation of the energy-gap shrinkage in heavily doped semiconductors is still controversial. It will be advantageous to have experimental data from a wider range of doped semiconductor materials to aid development of models describing gap-shrinkage phenomena. In this paper we report experimental data from optical studies concerning gap shrinkage in thin films of zinc oxide (ZnO) with carrier concentrations up to $n = 2 \times 10^{20} \text{ cm}^{-3}$ and compare the results with trends expected from available theoretical models.

There is general agreement that two competing phenomena are dominant in affecting the absorption edge in heavily doped semiconductors. First, the well-known Burstein-Moss band-filling effect which shifts positively the measured band-edge energy with increasing carrier concentration. In this case the measured optical gap E_m is the sum of the optical gap of the lightly doped material E_0 , plus that due to filling of the conduction band due to donors ΔE_{BM} , i.e., $E_m = E_0 + \Delta E_{\text{BM}}$. The second phenomenon which affects the optical absorption edge with increasing donor density is due to a change in the nature and strength of the interaction potentials between donors and the host crystal. This latter effect gives rise to a band-gap shrinkage and to some increased tailing of the absorption edge. In this case the measured optical gap is $E_m = E_0 + \Delta E_{\text{BM}} - \Delta E_g$, where ΔE_g is the gap shrinkage. The onset of the gap shrinkage can be

related to a semiconductor-metal transition accompanied by a merging of the donor and the conduction bands. It is usually assumed that the merging does not alter the *k* dependence of the conduction band (i.e., rigid shift of the band with no change in the electron effective mass¹). Thus the gap shrinkage can be deduced as the difference between the expected Burstein-Moss shift and the measured absorption edge shift: $\Delta E_g = \Delta E_{\text{BM}} - \Delta E_{\text{measured}}$. In a recent paper⁶ we have shown that ZnO films prepared by organometallic chemical vapor deposition and reactive (rf) magnetron sputtering exhibit an absorption edge shift ΔE_m which followed the Burstein-Moss model fairly well up to $n \approx 2 - 3 \times 10^{19} \text{ cm}^{-3}$. Above that critical carrier concentration the measured gap shift ΔE_m was always smaller than ΔE_{BM} . In this paper, we turn to the determination of the gap shrinkage ΔE_g as a function of carrier concentration up to $n = 2 \times 10^{20} \text{ cm}^{-3}$ and compare the energy dependence of ΔE_g with available theoretical models.

The samples analyzed had carrier concentrations ranging from 5×10^{17} to $2 \times 10^{20} \text{ cm}^{-3}$, a concentration range previously unobtainable for defect-doped ZnO. We include samples prepared by four distinct techniques: organometallic chemical vapor deposition⁷ (OMCVD), reactive rf magnetron sputtering⁸ (RRFMS), bias sputtering⁹ (BS), and reactive evaporation¹⁰ (RE). These films, deposited on glass substrates, were always polycrystalline, reasonably well oriented with the *c'* crystal axis almost normal ($\pm 10^\circ$) to the substrate. The films have shown *n*-type semiconducting properties due to stoichiometric changes of the growing film during deposition. Excess zinc or oxygen vacancies form donor states at 0.05 eV below the conduction band. The carrier concentrations have been deduced from Hall measurements at room tempera-

ture. Where undertaken, chemical analysis has shown only the presence of Zn and O in the films.

Transmission and reflectivity spectra of ZnO thin films have been measured at room temperature on a double beam spectrophotometer, with a clean pyrex glass substrate in the reference beam for transmission and an aluminium mirror for reflectivity. The effects of the glass substrate can thus be eliminated and the absorption calculated, using standard thin-film equations. At 0 K and low carrier density the absorption in a direct gap semiconductor is proportional to $(h\nu - E_0)^{1/2}$ for $h\nu$ not too large; at higher energy the actual band structure must be taken into account. At high temperature or at higher carrier concentration a low-energy tail modifies the absorption spectra at energies close to and below E_m , the optical gap. Indeed, as we show in Fig. 1, the experimental curves exhibit such a tail. The reflectivity spectra do not vary noticeably with the carrier concentration. Since the overall energy dependence of the curves does not change appreciably with increasing n we have used a single criterion for measuring E_m for all samples. In this method, as explained below, we modify the absorption by adding an empirical broadening which, from the results of Fig. 1, can be assumed to have an analytical form independent of the carrier concentration. We have chosen a Lorentzian-type broadening which has been shown to yield accurate results in other direct gap materials,¹¹ and which also reproduced the

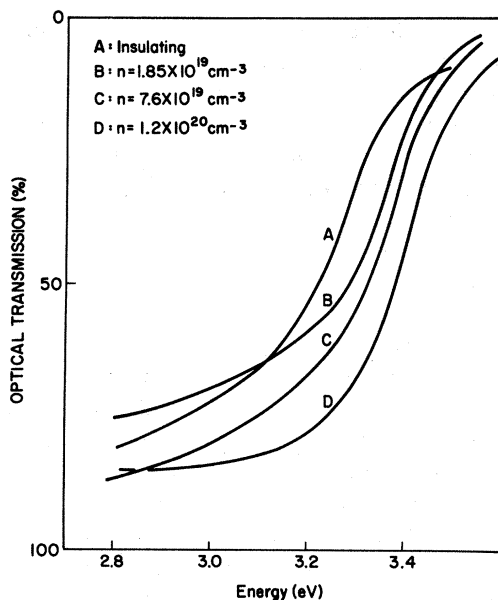


FIG. 1. Experimental transmission spectra of four ZnO thin films, measured at 300 K.

shape of the present experimental curves reasonably well. When such a broadening δ modifies α , then

$$\alpha \sim \{[(h\nu - E_m)^2 + \delta^2]^{1/2} + (h\nu - E_m)\}^{1/2},$$

and it can be readily shown that the maximum of $\partial\alpha/\partial(h\nu)$ occurs at $h\nu_1 = E_m + \delta/\sqrt{3}$. Also, the tangent to $\alpha(h\nu)$ at energy $h\nu_1$ intercepts the energy axis at $h\nu_2 = E_m - \sqrt{3}\delta$. Thus E_m is easily calculated from the measured value of $h\nu_1$ and $h\nu_2$, $E_m = (3h\nu_1 + h\nu_2)/4$. The previously reported values of E_m , used in the context of the Burstein-Moss model,⁶ together with some new results from samples prepared by other techniques, serve now to calculate the gap shrinkage, i.e., the difference between the theoretical Burstein-Moss shift and the absorption-edge shift measured at 300 K and referred to the insulating ZnO gap. In total, 21 samples with different histories and carrier concentrations have been examined. As shown in Fig. 2, this experimentally determined gap shrinkage does not depend on sample preparation; hence it represents a fundamental property of zinc oxide. No gap narrowing was observed below $n \approx 3 \times 10^{19} \text{ cm}^{-3}$. Above this carrier density a rapid increase in gap shrinkage occurs, which appears to be related to a semiconductor-metal transition. In many materials, this transition is observable as a disappearance of the conductivity activation energy.¹² This feature was not observed for these ZnO films, since the films are all polycrystalline, and the carrier mobility is dominated by grain boundary effects.⁷ However, the carrier concentration at which a semiconductor-metal transition is expected to occur in ZnO can be calculated from various theoretical models which all make use of the relation

$$n_c^{1/3} a^* = K, \quad (1)$$

where a^* is the donor radius, and K is a constant. The predicted value of K varies from 0.18 to 0.376 depending on the theoretical model.¹³ This relation yields the carrier concentration n_c which corresponds to delocalization of the donor states. In the effective-mass approximation the donor radius expressed in Å in ZnO is

$$a^* = \frac{\epsilon}{m^*} \frac{\hbar^2}{e^2} \approx 11.8, \quad (2)$$

where ϵ is the dielectric constant and m^* the electron effective mass of the material. With this value of a^* , and taking the Thomas-Fermi screening model, $K \approx 0.25$ (Ref. 13), Eq. (1) yields $n_c \approx 9.4 \times 10^{18} \text{ cm}^{-3}$. Other values of K give n_c

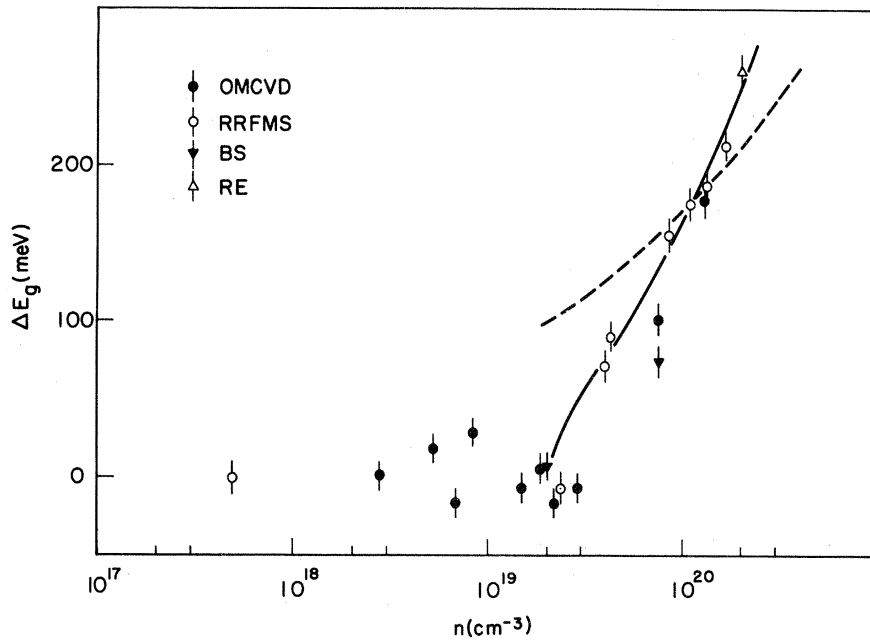


FIG. 2. Band-gap shrinkage in ZnO, measured at 300 K on samples of four different origins (see text).

values varying from 4.8×10^{18} to $2.2 \times 10^{19} \text{ cm}^{-3}$. Therefore, the onset of gap narrowing measured in ZnO occurs at a carrier concentration $n = 2 - 3 \times 10^{19} \text{ cm}^{-3}$ which falls in the range $n_c - 10n_c$ in agreement with theoretical predictions, and also with experimental evidence from other materials for the merging of the donor and conduction bands.¹⁴

The dependence of the gap shrinkage on carrier concentration has been considered recently.^{2,4,5} Most early calculations of the gap shrinkage (ΔE_g) neglected some of the factors which contribute to ΔE_g , and the agreement between experiment and calculations was fortuitous due to canceling effects. Recent model calculations^{2,5} are more complete, but only apply well at very high carrier densities, where $n \gg n_c$ as given by Eq. (1). In these calculations, which are all based on a weakly interacting electron-gas model, the gap shrinkage is proportional to $n^{1/3}$, at least in a first approximation. We have thus plotted in Fig. 2 (dashed line) the relation

$$\Delta E_g = An^{1/3}, \quad (3)$$

where A has been adjusted to give the measured value for ΔE_g at high n . For $n \approx 10^{20} \text{ cm}^{-3}$, $A \approx 3.6 \times 10^{-5} \text{ meV cm}^3$. Equation (3) has been used to represent results obtained for n -Ge (Ref. 15) and p -GaAs (Ref. 16) and reasonably good agreement with experimental data was obtained

with similar A values. However, in contrast, the agreement shown for ZnO in Fig. 2 is not good, although part of this disagreement may disappear for large n if the experimental data were obtained at 4 K and not 300 K, as zero Kelvin has been assumed in the calculations leading to this $n^{1/3}$ dependence of ΔE_g . The problems associated with the understanding of gap shrinkage are clearly illustrated in that Balkansky¹⁷ and Schmid⁴ have shown that Si:P and Si:As; Si:B also do not follow an $n^{1/3}$ dependence. Schmid noted that calculations based on the electron-gas model failed in their prediction of both the absorption line shape and gap shrinkage, and he analyzed his low-temperature interband absorption data with the empirical relation

$$\Delta E_g = B \left[\frac{n - n'}{n'} \right]^\gamma, \quad (4)$$

where n' is the carrier concentration at the onset of gap shrinkage, and B and γ are parameters. The solid curve of Fig. 2 has been calculated from Eq. (4) with the parameters shown in Table I. Table I also shows the parameters required to give the best fit to the 35-K data of Balkansky *et al.*,¹⁷ as well as the parameters used by Schmid for Si:As and Si:B (Ref. 4). It appears that the analytical form of Eq. (4) reproduces the observed experimental data quite well for at least two different materials. The difference in γ may be due to different

TABLE I. Parameters used to fit experimental gap shrinkages in various semiconductors using Eq. (4). n_c is the calculated critical carrier concentration corresponding to a metal-semiconductor transition.

Material	n' (cm^{-3})	B (meV)	γ	n_c (effective-mass approximation) (cm^{-3})	T (K)
Si:As ^a	6×10^{18}	14	0.8	4.6×10^{18} ^d	4–300
Si:B ^a	5×10^{18}	9	0.8		4–300
Si:P ^b	6×10^{18}	23	0.5	3.9×10^{18} ^d	35
ZnO ^c	2×10^{19}	75	0.55	9.4×10^{18}	300

^aReference 4.

^bOur calculations from data of Ref. 17.

^cThis work.

^dReference 18.

methods of reducing the experimental data into a gap shrinkage. The more important point is the direct relation between gap shrinkage and the semiconductor-metal transition. Also it appears from these results on Si and ZnO that the electron-gas models which lead to the $n^{1/3}$ dependence of ΔE_g are not appropriate at $n_c \leq n \leq 10n_c$ so that more detailed considerations are needed in this carrier concentration range. Unfortunately the empirical nature of Eq. (4) makes it difficult to compare the effects of different contributions to

ΔE_g such as dielectric screening, distribution of donor centers, etc. It is hoped the extension of gap-shrinkage measurements to materials such as ZnO will help to better quantify the physical source of gap shrinkage in heavily doped semiconductors.

We wish to express our thanks to D. Brodie (University of Waterloo) and K. Murti (Xerox Research Center of Canada) for giving us some of their ZnO samples to be used in this work.

¹R. A. Abram, G. J. Rees, and B. L. H. Wilson, *Adv. Phys.* **27**, 799 (1978).

²G. D. Mahan, *J. Appl. Phys.* **51**, 2634 (1980).

³J. Serre, A. Ghazali, and P. Leroux-Hugon, *Phys. Rev. B* **23**, 1979 (1981).

⁴P. E. Schmid, *Phys. Rev. B* **23**, 5531 (1981).

⁵K. F. Berggren and B. E. Sernelius, *Phys. Rev. B* **24**, 1971 (1981).

⁶A. P. Roth, J. B. Webb, and D. F. Williams, *Solid State Commun.* **39**, 1269 (1981).

⁷A. P. Roth and D. F. Williams, *J. Appl. Phys.* **52**, 6685 (1981).

⁸J. B. Webb, D. F. Williams, and M. Buchanan, *Appl. Phys. Lett.* **39** (8), 640 (1981).

⁹D. K. Murti, in *Proceedings of the Symposium on Sputtering*, National Research Council of Canada, Ottawa, 1981 (unpublished).

¹⁰D. E. Brodie, R. Singh, J. H. Morgan, J. D. Leslie, L. J. Moore, and A. E. Dixon, in *Proceedings of the 14th*

IEEE Photovoltaic Specialists Conference (The Institute of Electrical and Electronics Engineers, Inc., New York, 1980), p. 468.

¹¹A. P. Roth, W. J. Keeler, and E. Fortin, *Can. J. Phys.* **58**, 560 (1980).

¹²J. B. Webb and M. Sayer, *J. Phys. C* **9**, 4151 (1976).

¹³T. G. Castner, N. K. Lee, G. S. Cieloszyk, and G. L. Salinger, *Phys. Rev. Lett.* **34**, 1627 (1975).

¹⁴N. F. Mott, *Metal-Insulator Transitions* (Taylor and Francis, London, 1974), Chap. 6.

¹⁵A. A. Rogachev and N. I. Sablina, *Fiz. Tverd. Tela* (Leningrad) **8**, 866 (1966) [*Sov. Phys.—Solid State* **8**, 691 (1966)].

¹⁶H. C. Casey and F. Stern, *J. Appl. Phys.* **47**, 631 (1976).

¹⁷M. Balkansky, A. Azizu, and E. Amzullag, *Phys. Status Solidi* **31**, 323 (1969).

¹⁸K. F. Berggren, *Philos. Mag.* **27**, 1027 (1973).